




# PHOTONICS Research

## CsPbBr<sub>3</sub> perovskite quantum-dot paper exhibiting a highest 3 dB bandwidth and realizing a flexible white-light system for visible-light communication

KONTHOUJAM JAMES SINGH,<sup>1,2</sup>  XIAOTONG FAN,<sup>3</sup> ANNADA SANKAR SADHU,<sup>1,2</sup> CHUN-HO LIN,<sup>4</sup>  FANG-JYUN LIOU,<sup>1</sup> TINGZHU WU,<sup>3,7</sup>  YU-JUNG LU,<sup>5</sup> JR-HAU HE,<sup>6</sup> ZHONG CHEN,<sup>3</sup> TOM WU,<sup>4</sup> AND HAO-CHUNG KUO<sup>1,8</sup>

<sup>1</sup>Department of Photonics & Institute of Electro-Optical Engineering, College of Electrical and Computer Engineering, Taiwan Yang Ming Chiao Tung University, Hsinchu 30010, China

<sup>2</sup>International Ph.D. Program in Photonics (UST), College of Electrical and Computer Engineering, Taiwan Yang Ming Chiao Tung University, Hsinchu 30010, China

<sup>3</sup>Department of Electronic Science, Fujian Engineering Research Center for Solid-State Lighting, Xiamen University, Xiamen 361005, China

<sup>4</sup>School of Materials Science and Engineering, University of New South Wales, Sydney, NSW 2052, Australia

<sup>5</sup>Research Center for Applied Sciences, Academia Sinica, Taipei 11529, China

<sup>6</sup>Department of Materials Science and Engineering, City University of Hong Kong, Kowloon Tong, Hong Kong, China

<sup>7</sup>e-mail: wutingzhu@xmu.edu.cn

<sup>8</sup>e-mail: hckuo@faculty.nctu.edu.tw

Received 15 June 2021; revised 6 September 2021; accepted 6 September 2021; posted 29 September 2021 (Doc. ID 434270); published 10 November 2021

We propose a flexible white-light system for high-speed visible-light communication (VLC) applications, which consists of a semipolar blue InGaN/GaN single-quantum-well micro-light-emitting diode (LED) on a flexible substrate pumping green CsPbBr<sub>3</sub> perovskite quantum-dot (PQD) paper in nanostructure form and red CdSe QD paper. The highest bandwidth for CsPbBr<sub>3</sub> PQD paper, 229 MHz, is achieved with a blue micro-LED pumping source and a high data transmission rate of 400 Mbps; this is very promising for VLC application. An 817 MHz maximum bandwidth and a 1.5 Gbps transmission speed are attained by the proposed semipolar blue micro-LEDs. The proposed flexible white light system and the high-bandwidth PQD paper could pave the way for VLC wearable devices. © 2021 Chinese Laser Press

<https://doi.org/10.1364/PRJ.434270>

### 1. INTRODUCTION

Through technological advances, light-emitting diode (LED)-based systems have been commercialized and are now widely used in applications such as large displays, traffic lights, indoor and street lighting, automobiles, cell phones, and liquid-crystal displays [1–3]. Recently, white-light-emitting materials have attracted considerable attention owing to their potential use in LEDs, lighting, communications, and, especially, flexible display devices. White-light systems based on micro-LEDs and color converters such as quantum dots (QDs) are becoming more prominent in visible-light communication (VLC) applications. Furthermore, organic optoelectronic components are now being used in VLC systems because they are cheaper and more environmentally friendly, portable, and flexible than traditional silicon-based devices; moreover, they can be mass-produced [4–9]. Application of organic optoelectronic

components to VLC systems will allow such systems to be incorporated into wearable fabrics and industrial products.

Regular white-light-emitting diodes (WLEDs) for lighting can be used for high-speed modulation; hence, they can be simultaneously applied to wireless data transmission at no major cost. However, WLED modulation bandwidths are significantly limited by the long response times of the color-conversion materials. Additionally, factors such as the dimming and flickering of color-conversion materials should be considered when designing modulation techniques. For example, in on–off keying (OOK) modulation techniques, LED devices are turned on or off depending on the data bit, where the on and off states present “1” and “0” bits, respectively. The shorter the fluorescence lifetime, the faster the luminous intensity drop to a characteristic point in the “0” state. For clear and rapid data representation, the switching time between “0” and “1”

should be as short as possible, and the “0” and “1” luminous intensities should differ considerably; if such characteristics are realized, more data can be accurately reproduced in a unit time.

Full-color flexible displays can be fabricated using a flexible blue LED chip and color converters or yellow-light-emitting phosphors. However, the conventional white-light generation approach is unsuitable for flexible displays. Thus, inorganic white-light-emitting phosphors must be used, which are hard and brittle [10]. Quantum dots (QDs) have very promising application as color converters, especially because of their narrow full-width at half-maximum (FWHM) of approximately 30 nm; this affords high color purity and a tunable bandgap that is governed by the quantum size effect; further, the emission tunability is efficient and influenced by the QD composition [11–13]. Moreover, the non-radiative energy transfer between QDs and micro-LED enhances the color conversion efficiency of the full-color micro-LED devices [14]. Importantly, QD solutions can be cast on flexible substrates for use in flexible displays. For WLEDs, the fluorescence lifetimes of the color-conversion materials have a more significant influence on the resultant VLC. Unfortunately, the modulation bandwidth of common CdSe/ZnS QDs is limited to  $\sim 3$  MHz [15], which is far below VLC requirements.

Halide perovskite QDs (HPQDs) have evolved as an alternative to CdSe/ZnS QDs because of their outstanding characteristics, which derive from their narrower FWHM (below 30 nm). This property yields greater color purity, higher photoluminescence quantum yield (approaching 100%), more convenient synthesis, and lower manufacturing costs than conventional QDs [16,17]. In particular, PQDs exhibiting short carrier recombination lifetimes and narrow spectral linewidths have attracted interest because they can be used to develop white-light VLC systems with considerably higher modulation bandwidth than CdSe/ZnS QDs [18]. Therefore, HPQDs have been used in different electronic and optoelectronic applications, such as in photodetection, photovoltaics, and photoemission; however, they are usually employed as active materials or color converters in LEDs [19–22].

The highest reported modulation bandwidth for a white-light system combining a micro-LED with PQDs is low, at 85 MHz [23]. Therefore, increasing the bandwidth of the VLC white-light source is essential, and considerable efforts have been made to increase the bandwidths of both color converters and blue LEDs [24,25]. Recently, Xia *et al.* reported ultrastable perovskite nanocrystals for underwater optical wireless communication with a maximum bandwidth of 180 MHz [26]. In several systems, the bandwidth has been increased from  $\sim 3$  to  $\sim 11$  MHz, with the lifetime being reduced from  $\sim 68$  to  $\sim 11$  ns. To realize a high-bandwidth white-light system, high-bandwidth PQDs in combination with semipolar blue micro-LEDs are preferred, with the latter exhibiting a high modulation bandwidth owing to their smaller size, shorter carrier lifetime, and higher current density [27]. To date, no PQDs with modulation bandwidths exceeding 200 MHz have been developed; therefore, development of a high-performance VLC system combining high-bandwidth micro-LEDs with high-bandwidth PQDs is necessary.

In this study, we propose a high-performance flexible white-light system that has immense potential for VLC applications. This proposed system is constructed with nanostructured green-emitting CsPbBr<sub>3</sub> PQD paper, red-emitting CdSe QD paper, and a semipolar blue micro-LED. The semipolar micro-LED has 817 MHz maximum bandwidth and 441 nm peak emission wavelength. The green PQD paper has 229 MHz maximum bandwidth, the highest value reported to date, while the observed bandwidth for the red CdSe QDs is below 25 MHz. The data rates of the semipolar device and the green PQD paper are 1.5 Gbps and 400 Mbps, respectively, and the proposed PQD-based flexible white-light system can also achieve a maximum 3 dB bandwidth of 95.5 MHz. These results indicate that our proposed white-light system is very promising for VLC applications.

## 2. EXPERIMENT

### A. Preparation of the Cellulose Nanocrystal Suspension

To prepare the cellulose nanocrystal suspension, 168 mg freeze-dried cellulose nanocrystals (CNCs) were mixed with 16 mL anhydrous dimethylformamide solution. The mixed solution was then sonicated for approximately 2 h.

### B. Preparation of the CsPbBr<sub>3</sub> PQD Paper

To prepare the Cs-oleate solution, 1.05 g Cs<sub>2</sub>CO<sub>3</sub> was mixed with a mixture of 52 mL 1-octadecene (ODE) and 3.25 mL oleic acid (OA) solution. The resultant solution was then dried at 120°C for 1 h and heated at 150°C under a N<sub>2</sub> atmosphere until all Cs<sub>2</sub>CO<sub>3</sub> molecules reacted with the OA. The solution was maintained at 150°C before injection to prevent solidification of the Cs-oleate. To prepare the CsPbBr<sub>3</sub> PQD solution, 0.89 mg PbBr<sub>2</sub> was mixed with 65 mL ODE solution and the solution was cured at 120°C for 1 h. Then, a mixture of 6.5 mL OA solution and 6.5 mL oleylamine solution was injected into the PbBr<sub>2</sub> solution under a N<sub>2</sub> atmosphere at 120°C. When the PbBr<sub>2</sub> salt had fully dissolved, the temperature was increased to 180°C, and approximately 4 mL prepared Cs-oleate solution was injected to obtain the CsPbBr<sub>3</sub> solution. To prepare the CsPbBr<sub>3</sub> PQD paper, 1.5 mL CsPbBr<sub>3</sub> solution was added to 10.5 mL CNC suspension; the solution was then sonicated for 2 h. The mixed solution was filtered through a filter membrane using a vacuum-pump setup. The CNC/CsPbBr<sub>3</sub> PQD material accumulated at the top of the filter membrane for 24 h under continuous vacuum pumping. The CsPbBr<sub>3</sub> PQD paper in nanostructure form was then separated from the filter membrane.

### C. Preparation of the CdSe QD Paper

To prepare the CdSe QDs, 1 mmol CdO, 15 mL ODE, and 1.44 mmol OA were mixed and then heated to 300°C under a N<sub>2</sub> flow to obtain a clear colorless solution. Then, 10 mL Se stock solution was added and the temperature was reduced to 290°C; this temperature was maintained for 40–50 s to allow CdSe QD growth. Ethanol was then added to the solution at room temperature. Next, the solution was centrifuged and washed several times with ethanol, and dried for 12 h in an oven at 70°C. The obtained QDs were then dispersed in cyclohexane for use. To prepare the CdSe QD paper, the same

preparation process as for the CsPbBr<sub>3</sub> PQD paper was used, but 2 mL CdSe QD solution was mixed with 14 mL CNC.

#### D. Fabrication of the Semipolar Micro-LED Device

The structure and fabrication process of the micro-LED device were similar to those employed in our previous studies [28–30]. Metal organic chemical vapor deposition (MOCVD) was used to grow semipolar (20–21)-oriented GaN layers on patterned sapphire substrates. To directly develop GaN on a sapphire wafer, we employed an advanced orientation-controlled epitaxy method; this is a simple epitaxy technique involving MOCVD for developing semipolar GaN.

For *c*-plane devices, a large polarization field exists across the quantum wells (QWs). This causes a severe quantum-confined stark effect (QCSE), resulting in less overlap of the electron–hole wave function and an increased recombination lifetime. These issues can be overcome by growing semipolar planes with a high inclination angle, such as (20–21) [31]. Semipolar blue micro-LEDs have gained substantial attention owing to their specific mechanical properties and device performance, such as critical thickness, high efficiency, low efficiency droop, and low thermal droop [32–34]. In addition, both the efficiency droop and thermal droop can be minimized by the growth of thick single-QW (SQW) structures of semipolar planes.

In this study, semipolar (20–21) GaN was developed after the substrates were prepared. Ge doping was then employed in the initial epitaxy phase to produce stacking-fault-free semipolar GaN. A bulk GaN layer was formed by depositing undoped GaN after the Ge-doped GaN strips had coalesced. The micro-LED epitaxial structure consisted of an n-GaN layer, an InGaN/GaN SQW as the active region, and a p-type GaN layer. The micro-LED was fabricated through deposition of an indium tin oxide (ITO) layer, followed by mesa etching of the ITO film using hydrochloric acid and an inductively coupled plasma reactive ion-etching process (to form a p-type ohmic contact). This process was accompanied by thermal annealing to provide a better current-spreading layer. Finally, the electrodes were deposited with a Ti/Al/Ti/Au structure, after which an Al<sub>2</sub>O<sub>3</sub>–SiO<sub>2</sub> passivation layer was formed to prevent leakage current due to sidewall defects [35,36]. The Al<sub>2</sub>O<sub>3</sub> passivation layer was grown through atomic layer deposition, and the SiO<sub>2</sub> passivation layer was grown using

plasma-enhanced chemical vapor deposition. Finally, Ti/Al/Ti/Au was deposited again as the pad metal and sidewall reflector. Figures 1(a) and 1(b) show the resulting 2D structure of the manufactured semipolar micro-LED and a corresponding optical microscopy image of the semipolar micro-LED array, respectively.

#### E. Fabrication of the Flexible White-Light System

A flexible white-light system was developed using a flexible blue micro-LED and CsPbBr<sub>3</sub> green PQD paper with CdSe red QD paper. The white-light system fabrication process is shown in Fig. 2. The flexible micro-LED was fabricated using a polyimide (PI) substrate covered with copper-foil shielding tape, where the latter was subjected to photolithography and wet etching to establish electrical conduction. Note that PI substrate was used because of its favorable characteristics, such as high heat resistance and thermostability. The micro-LED flip-chip was bonded on the PI substrate using a silicone-based electrically conductive anisotropic adhesive to maintain the electrical conductivity between the chip metal contact and the AuSn solder on the substrate; this increased the system flexibility. Bonding was performed at 230°C and 2.5 kilogram force (kgf). For the color converter, CsPbBr<sub>3</sub> PQD paper and CdSe QD paper were prepared as shown in Fig. 2. These papers were adhered to the top of the micro-LED with flexible substrate using an adhesive. For sticking QD paper to the micro-LED, we used epoxy resin adhesive, as it is colorless and transparent and it will not affect the color conversion of QDs. This adhesive is preferable because it has high thermal conductivity allowing for more heat dissipation from the device, thereby prolonging its lifetime. The white-light system was then complete.

### 3. RESULTS AND DISCUSSION

Figure 3 shows the structural and optical characteristics of the fabricated PQD paper. In contrast to the standard phase of CsPbBr<sub>3</sub> (ICSD-29073), the X-ray diffraction (XRD) patterns in Fig. 3(a) show that the PQDs have a cubic phase. Note that the XRD peak at 11.86° is not associated with the CsPbBr<sub>3</sub> PQDs but may correspond to PbBr<sub>2</sub> nanoparticles. The transmission electron microscopy (TEM) images for lesser resolution (×400,000) and high resolution (×5,000,000) along

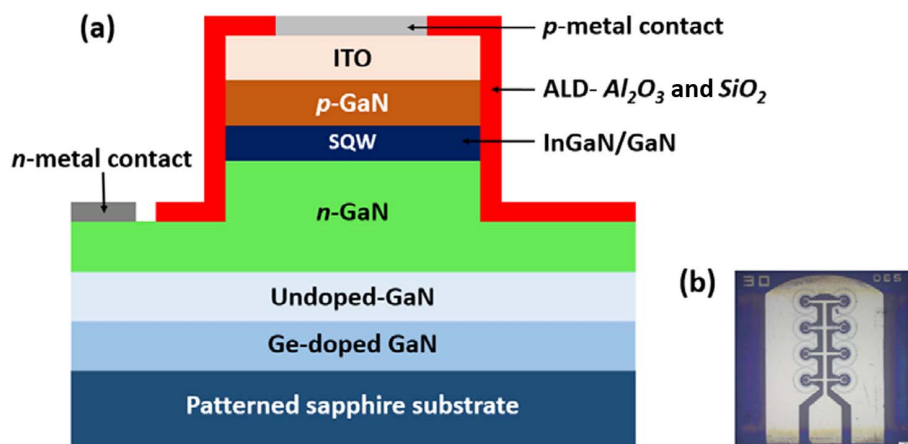
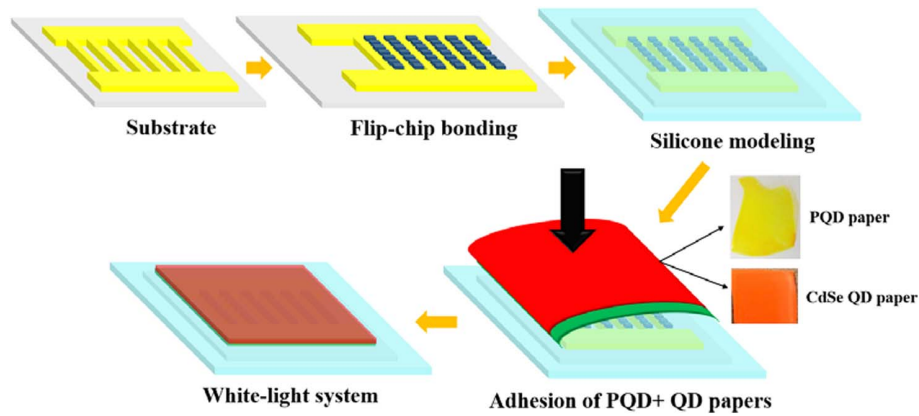


Fig. 1. (a) Schematic of semipolar micro-LED structure; (b) optical microscopy image of micro-LED.



**Fig. 2.** Fabrication of white-light system.

with the size distribution of the PQDs are shown in Fig. 3(b). It can be seen that the average diameter of the PQDs is  $9 \pm 2$  nm confirming the formation of QDs. The  $\text{Al}_2\text{O}_3$  passivation layer has been deposited on the top of the PQDs paper to prevent the surface from oxidation, thereby improving the stability of the PQDs paper. The ultraviolet–visible (UV–vis) absorption and photoluminescence (PL) spectra of the green PQD paper are shown in Fig. 3(c), revealing a peak emission wavelength of 528 nm and an FWHM of 39 nm. The UV absorption spectra show that the blue micro-LED effectively pumped the PQD paper.

The optical characteristics of the fabricated micro-LED, PQD paper, and white-light system were analyzed. The light–current–voltage ( $L$ – $I$ – $V$ ) curve for the semipolar micro-LED at a 25°C operating temperature is shown in Fig. 4(a). The semipolar micro-LED had a forward voltage of approximately 3.45 V, suggesting electrical characteristics comparable to those

of  $c$ -plane devices. In detail, this micro-LED had 4.5 mW light output power at a 72 mA injection current. The light output power produced by the semipolar micro-LED was sufficient to pump the PQD paper and CdSe QD paper to realize the white-light system. Figure 4(a) inset is an optical image of the illumination from the semipolar micro-LED array. The electroluminescence (EL) spectra of the semipolar micro-LED attained under different driving currents are shown in Fig. 4(b). A 441 nm peak emission wavelength and a narrow FWHM of 28.19 nm were observed under a 72 mA injection current. This narrow FWHM suggests that the epitaxy produced a high-quality structure and was therefore responsible for the delivery of pure emitted light, matching colors, and a wide color gamut. This outcome indicates that the epitaxial features of the semipolar plane were similar to those of  $c$ -plane devices. However, the FWHM increased with the current, possibly because of the band-filling effect in the SQW. A slight blueshift in

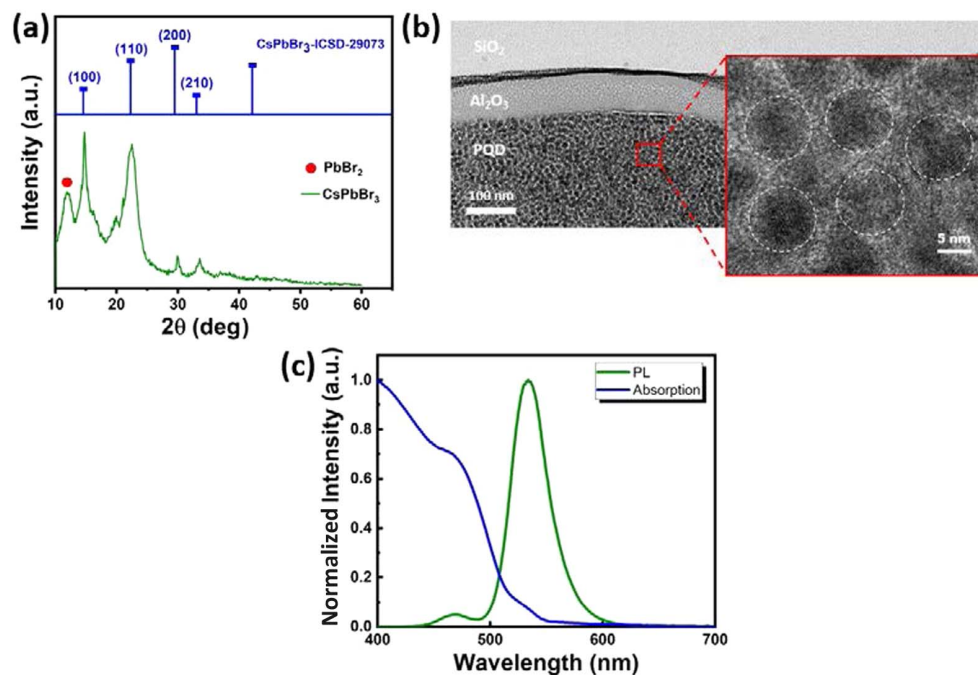


**Fig. 3.** (a) XRD patterns, (b) TEM images; inset:  $\times 5,000,000$  resolution, and (c) PL and UV absorption spectra of the PQD paper.

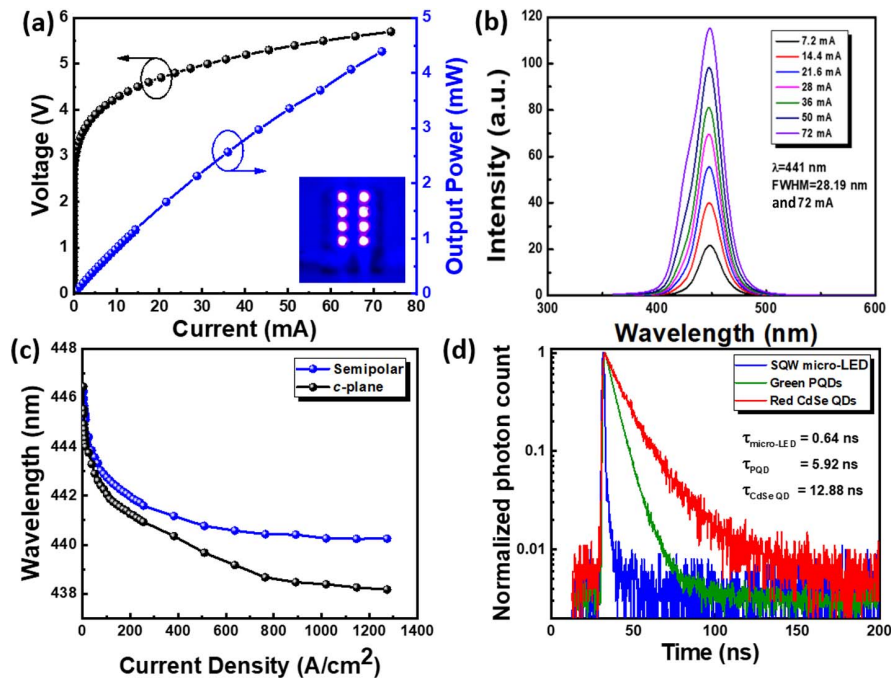


**Fig. 4.** (a)  $L$ - $I$ - $V$  characteristics of semipolar micro-LED; (b) EL spectra of semipolar micro-LED with increasing injection current; (c) peak wavelengths of  $c$ -plane and semipolar micro-LEDs for 1–1200  $A/cm^2$  current density; (d) TRPL curves for semipolar micro-LED and PQD and CdSe QD papers.

the EL spectrum was observed as the injection current increased from 7.2 mA; the wavelength stabilized after 72 mA. This blue-shift can be attributed to the reduced polarization-related electric fields in the SQWs grown on the semipolar orientation, which reduced the QCSE.

The peak wavelength shifts of the  $c$ -plane and semipolar micro-LEDs in response to injection current density variation from 1 to 1200  $A/cm^2$  are shown in Fig. 4(c). The peak wavelength shifts for the  $c$ -plane and semipolar devices were 8 and 6 nm, respectively. The semipolar-device peak wavelength stabilized after 1014  $A/cm^2$ ; however, even after 1200  $A/cm^2$ , the  $c$ -plane device did not exhibit any wavelength stability. In addition, as the injection current density increased, the semipolar device exhibited a smaller peak shift and stabilized faster than the  $c$ -plane device, indicating greater overlap in the electron-hole wave function and a reduced field of polarization.

Time-resolved photoluminescence (TRPL) was employed to investigate the carrier lifetimes of both the semipolar micro-LED and PQD paper as shown in Fig. 4(d). The photoluminescence (PL) decay curves were fitted using a double-exponential decay function, and the average lifetime ( $\tau_{avg}$ ) was estimated using the following equation:

$$\tau_{avg} = \frac{A_1\tau_1 + A_2\tau_2}{A_1 + A_2}, \quad (1)$$

where  $A$  and  $\tau$  are the amplitude and lifetime, respectively. The average PL lifetimes calculated for the semipolar micro-LED, PQD paper, and CdSe QD paper were 0.64, 5.92, and 12.88 ns, respectively. The semipolar device had a shorter lifetime because of the weak polarization-related electric field and large overlap of the electron-hole wave function, which yielded

a faster carrier recombination lifetime [32]. The QCSE reduction in the semipolar device yielded faster carrier transport and a shorter recombination lifetime, resulting in a weaker phase-space filling effect. Therefore, the semipolar micro-LED can achieve a high modulation bandwidth owing to its faster carrier recombination lifetime. Similarly, the PQD paper had a shorter carrier lifetime than those reported in other studies, while also being considerably shorter than those of phosphors [microsecond to millisecond ( $\mu$ s–ms) range] [23,37,38]. This shorter carrier lifetime is attributable to the quantum confinement effect, which yields faster radiative recombination. Faster carrier recombination can correspond to a higher 3 dB modulation bandwidth as reported by many researchers. However, the CdSe QD-paper carrier recombination lifetime is insufficient to independently achieve high bandwidth for VLC applications. Therefore, semipolar micro-LEDs and PQDs have considerable potential for VLC applications.

To realize a flexible white-light system, green-emitting PQD paper and red-emitting CdSe QD paper were used to form a color converter and placed on top of the semipolar blue micro-LED with flexible substrate. Figure 5(a) shows the EL spectrum of the white light generated from the flexible white-light system as the micro-LED drive current increased from 7.2 to 72 mA. This spectrum also shows the green and red light emissions from the PQD and CdSe QD papers, respectively, which had peak wavelengths of 528 and 625 nm, respectively; these results confirm the white-light generation. Figure 5(a) inset shows a flexible white-light system with high white-light illumination suitable for application in VLC wearable devices.

In addition to its potential for VLC applications, the PQD-based flexible white-light system reported herein displays a wide

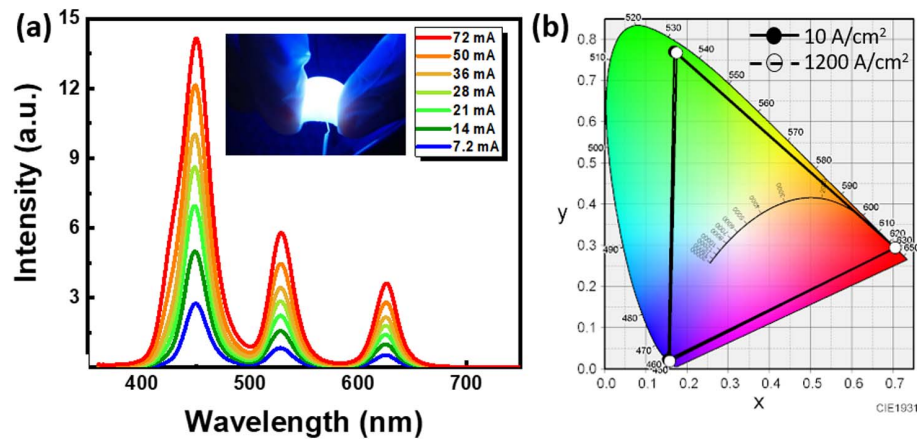


**Fig. 5.** (a) White-light spectrum generated using semipolar micro-LED and PQD and CdSe QD papers. Inset: photograph of flexible white-light system. (b) Color gamut of white-light system according to CIE 1931 color space under various current densities.

range of color characteristics and excellent color stability, which is very promising for display applications. Figure 5(b) shows the color performance of the white-light system created using the semipolar blue micro-LED with PQD paper and CdSe QD paper under driving conditions from 10 to 1200 A/cm<sup>2</sup>, according to the Commission Internationale de L'Éclairage (CIE) 1931 color space. The white-light system demonstrated a wide color gamut owing to the narrow EL spectrum, achieving 98.7% of the National Television Standards Committee (NTSC) space and 91.1% Rec. 2020 of the CIE 1931 color space. The color gamut of the white-light system remained almost unchanged with increasing injection current density owing to the wavelength stability. Note that the light extraction efficiency of the white-light system can be further increased through, for example, optimization of the PD or QD synthesis, the micro-LED device structure, or the on-chip setup.

The experimental setup used to measure the 3 dB modulation bandwidth is shown in Fig. 6. The measurement was performed using a vector network analyzer (Keysight E5071C) by supplying an alternating current to a direct-current bias tee, which was used to drive the micro-LED. The micro-LED then pumped the PQD + CdSe QD papers to emit white light, which was focused using lenses and detected by a photodetector (SPA-3, DC -2 GHz). The photodetector converted the light signal into an electrical signal and returned it to the network analyzer for analysis of the frequency response. Before measuring the modulation bandwidth of the white-light system, we measured the bandwidths of the semipolar micro-LED, PQD paper, and CdSe QD paper to analyze their individual transmission characteristics. To measure the VLC characteristics of the semipolar micro-LED, we collected the blue light from the micro-LED directly using the photodetector through an optical fiber. However, for the PQD paper and CdSe QD

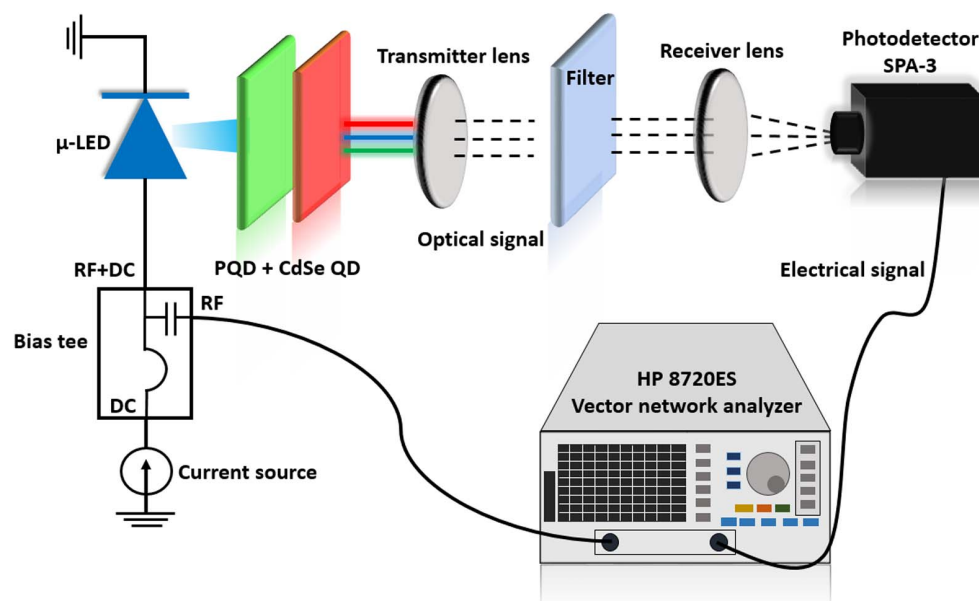


**Fig. 6.** Schematic of experimental setup for VLC bandwidth measurement.

paper, the green and red lights from the samples were detected by the photodetector after they had passed through an optical filter; this approach was used to filter out any remnant blue light from the micro-LED. The data rates of the semipolar micro-LED and PQD paper were measured to analyze the data transmission characteristics. For this measurement, an Anritsu MP1800A system was used to produce a back-to-back non-return-to-zero on-off key (NRZ-OOK)  $2^7 - 1$  pseudorandom bit sequence (PRBS-7), and a Tektronix DPO 7354C oscilloscope was used to record eye diagram results.

Figure 7 shows the results of the frequency response measurement and the extracted 3 dB modulation bandwidth for the flexible semipolar micro-LED, PQD paper, CdSe QD paper, and white-light system with increasing injection current at a transmission distance of 25 cm. The 3 dB bandwidth increased with the injection current; this can be attributed to the carrier lifetime reduction at higher injection current density. For the semipolar micro-LED, the carrier lifetime decreased with increasing injection current density in the active region, owing to the built-in electric-field screening effect. The semipolar blue micro-LED had a maximum 3 dB bandwidth of 817 MHz corresponding to an injection current of 113 mA as shown in Fig. 7(a); this is promising for VLC applications.

The measured modulation bandwidth for the semipolar blue micro-LED was higher than that of the green-emitting semipolar micro-LED [34]. The short average carrier lifetime of the semipolar micro-LED was consistent with the measured frequency bandwidth. The eye diagram of the semipolar micro-LED is shown in Fig. 7(a) inset. A maximum data rate of 1.5 Gbps was achieved owing to the sufficiently high 3 dB bandwidth. Note that, for micro-LEDs, the carrier recombination lifetime is related to the recombination rate, as a higher recombination rate shortens the carrier lifetime. The relationship is expressed as

$$\tau = \frac{\Delta n}{R} = \frac{1}{B(n_o + p_o + \Delta n)}, \quad (2)$$

where  $R$  is the net recombination rate;  $B$  is the recombination constant;  $n_o$  and  $p_o$  are the equilibrium electron and hole concentrations, respectively; and  $\Delta n$  is the excess carrier concentration. The semipolar micro-LED recombination rate is higher because of the reduced QCSE, which reduces the carrier

recombination lifetime. The 3 dB frequency bandwidth is related to the carrier lifetime through the following relation:

$$f_{-3\text{dB}} = \frac{\sqrt{3}}{2\pi\tau} = \frac{\sqrt{3}}{2\pi} \left( \frac{1}{\tau_r} + \frac{1}{\tau_{nr}} + \frac{1}{\tau_{RC}} \right), \quad (3)$$

where  $\tau_r$  is the radiative recombination lifetime,  $\tau_{nr}$  is the non-radiative recombination lifetime, and  $\tau_{RC}$  is the resistance-capacitance (RC) time constant. Hence, to enhance the modulation bandwidth, it is preferable to shorten  $\tau_r$ , but not  $\tau_{nr}$ . The measured 3 dB bandwidth of the green-emitting PQD paper was 229 MHz under a 113 mA injection current as shown in Fig. 7(b); this is the highest bandwidth reported for PQDs to date. The high-frequency response of the white-light system was attributed to the high-bandwidth PQD paper. Figure 7(b) inset shows the eye diagram of the PQD paper at a 400 Mbps data transmission rate; this is also the highest value reported to date. The high bandwidth and high data transmission rate were attributed to the short carrier recombination lifetime of the nanostructured PQD paper.

The differential carrier lifetime  $\tau_{\text{diff}}$  is related to the modulation bandwidth as follows:

$$\frac{1}{\tau_{\text{diff}}} = 2\pi f_{3\text{dB}}. \quad (4)$$

The TRPL data indicate the carrier lifetime, but not the differential carrier lifetime; however, the latter is usually 2–3 times shorter than the former. Consequently, a shorter carrier lifetime induces a shorter differential carrier lifetime and, as a result, a greater modulation bandwidth. Therefore, the high bandwidths of the semipolar micro-LED and PQD paper can be successfully explained by referring to the above explanation.

In a comparison of the PQD paper prepared with cellulose with a typical PQD film prepared through film-casting, the bandwidth of the nanostructured PQD paper was much higher than that of the PQD film as shown in Fig. 7(b). The method for the preparation of CsPbBr<sub>3</sub> PQD solution is similar in both cases. For making PQD paper, we mixed the PQD solution with cellulose nanocrystals (CNCs) suspension before casting it into PQD paper; however, for film casting PQD film, we made it by mixing PQD solution with PMMA solution. The PQD-film bandwidth was found to be 111 MHz; hence, the high bandwidth of the PQD paper is suitable for achieving high-speed VLC. This outcome implies that the nanostructure

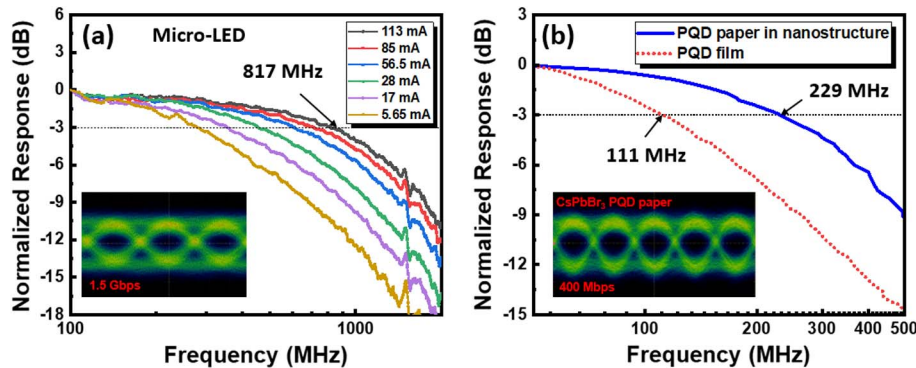


**Fig. 7.** (a) Frequency responses for semipolar blue micro-LED; inset: eye diagram. (b) Comparison of bandwidth of PQD paper in nanostructure with that of PQD film; inset: eye diagram for PQD paper.

**Table 1. Overview of Reported QDs for VLC**

Materials Type	Decay Lifetime ( $\tau$ )	Bandwidth	Data Rate	References
CsPbBr <sub>3</sub> PQDs paper	5.92 ns	229 MHz	400 Mbps	This work
CsPbBr <sub>3</sub> nanocrystals	5.93 ns	180 MHz	185 Mbps	[26]
CsPbBr <sub>1.8</sub> I <sub>1.2</sub> PQDs	43.74 ns	70 MHz	150 Mbps	[23]
CsPbBr <sub>3</sub> PQDs in CsPb <sub>4</sub> Br <sub>6</sub> matrix	–	24.6 MHz	364 Mbps	[39]
AgInS <sub>2</sub> /ZnS QDs	77 ns	5.4 MHz	–	[40]
CdSe/ZnS QDs	17.24 ns	23.1 MHz	–	[41]
CsPbBr <sub>3</sub> -in-Cs <sub>4</sub> PbBr <sub>6</sub> QDs	7 ns	41 MHz	380 Mbps	[42]
CdSe/ZnS QDs	26.31 ns	2.70 MHz	–	[15]

has a higher recombination rate than the bulk and hence a higher modulation bandwidth. The PQD-based white-light system also displayed a frequency bandwidth of 95.5 MHz at a 113 mA injection current. For measuring the bandwidth of the white light system, we removed the filter so that we can get white light to be detected by the photodetector. The modulation bandwidth of the CdSe QD paper was also measured but was found to be less than 25 MHz, which is quite low compared to that of the PQD paper. The high bandwidth of the white-light system was attributed to the high bandwidths of both the semipolar micro-LED and PQD paper. However, we believe that the modulation bandwidth of the white-light system was limited by the low bandwidth of the red CdSe QD paper, and that the system bandwidth can be further improved by optimizing the red component. These results confirm that PQDs enhance the modulation characteristics of white-light systems; in the future, PQDs can be further optimized for increased bandwidth.

Table 1 summarizes the results of studies investigating the use of QDs for VLC; the QD bandwidths are not remarkably high. Figure 8 shows various results for the 3 dB bandwidth benchmark as a function of current, as many researchers have attempted to increase the QD bandwidth. For example, Leitão *et al.* proposed a micro-LED-pumped inorganic PQD color converter for VLC with a 24.6 MHz bandwidth and 364 Mbps free-space data communication speed [39]. In 2018, Mei *et al.* reported a 70 MHz bandwidth for CsPbBr<sub>1.8</sub>I<sub>1.2</sub> PQDs with

150 Mbps transmission speed [23]. However, the reported CdSe QD bandwidth is low, having values of 2–25 MHz [15,24]. In 2016, Ruan *et al.* demonstrated AgInS<sub>2</sub>/ZnS QDs with an improved bandwidth of 5.4 MHz, higher than that of commercial YAG:Ce phosphor, for VLC [40]. Recently in 2021, Xia *et al.* demonstrated ultrastable perovskite nanocrystals with a maximum bandwidth of 180 MHz and a data rate of 185 Mbps for underwater optical wireless communication [26]. To the best of our knowledge, this paper reports the highest 3 dB bandwidth of 229 MHz, corresponding to a 113 mA injection current and achieved by PQDs.

The use of a white-light system for VLC applications has been reported in various studies. In 2018, Mei *et al.* developed a high-bandwidth white-light system by combining a micro-LED with PQDs having an 85 MHz maximum modulation bandwidth under an 80 mA injection current [23]. Further, Yeh *et al.* proposed a phosphor-based white-light system with a bandwidth that can be increased to 12 MHz [43]. Haicheng *et al.* reported a white-LED system using CdSe/ZnS QDs with a 637.6 MHz modulation bandwidth [41]. However, for VLC applications, CdSe QDs are not optimal; hence, researchers have begun to use PQDs to achieve further advancements. Because very few studies have investigated white-light systems fabricated using micro-LEDs and PQDs, our study should be of significant interest to researchers interested in VLC. In addition, this work should encourage the development of other white-light systems with considerably higher modulation bandwidth.

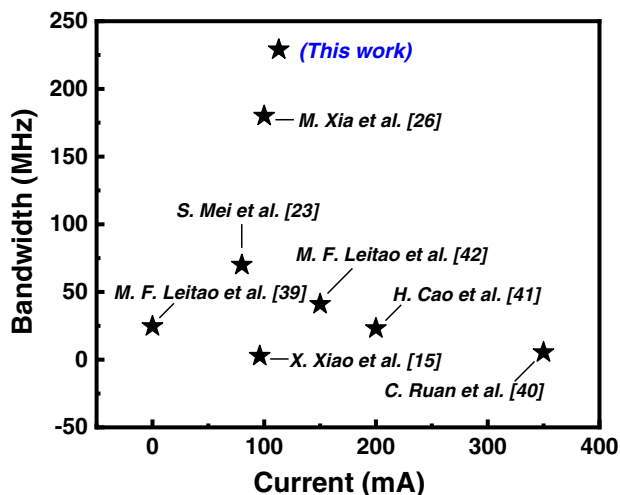


**Fig. 8.** Benchmark of 3 dB bandwidth for QDs with applied current.

## 4. CONCLUSIONS

In this study, we demonstrated the potential of nanostructured green CsPbBr<sub>3</sub> PQD paper as a color converter in a white-light system containing a semipolar blue InGaN/GaN micro-LED. The PQD paper used in this study achieved the highest modulation bandwidth reported to date of 229 MHz with a 400 Mbps data transmission rate, and the semipolar micro-LED had an 817 MHz modulation bandwidth with a 1.5 Gbps data rate. The proposed PQDs-based flexible white-light system can also achieve a maximum 3 dB bandwidth of 95.5 MHz. The short carrier lifetimes of the PQD paper and semipolar micro-LED allowed high bandwidths for the flexible white-light system. However, the bandwidth of the white-light system is limited by the use of low-bandwidth CdSe QD paper, which can be further improved in future by optimizing the red component. Hence, the proposed PQD-based flexible white-light system has considerable potential and it could pave



the way for various VLC applications including wearable devices.

**Funding.** Ministry of Science and Technology, Taiwan (108-2221-E-009-113-MY3, 110-2124-M-A49-003-); National Natural Science Foundation of China (11904302); Major Science and Technology Project of Xiamen (3502ZZ20191015).

**Acknowledgment.** The authors thank Pengfei Tian of Fudan University for the helpful discussion.

**Disclosures.** The authors declare no conflicts of interest.

**Data Availability.** Data underlying the results presented in this paper are not publicly available at this time but may be obtained from the authors upon reasonable request.

## REFERENCES

- J. Cho, J. H. Park, J. K. Kim, and E. F. Schubert, "White light-emitting diodes: history, progress, and future," *Laser Photon. Rev.* **11**, 1600147 (2017).
- D. Zhu and C. J. Humphreys, "Solid-state lighting based on light emitting diode technology," in *Optics in Our Time*, M. D. Al-Amri, M. El-Gomati, and M. S. Zubairy, eds. (Springer International Publishing, 2016), pp. 87–118.
- A. Žukauskas, M. S. Shur, and R. Gaska, "Light-emitting diodes: progress in solid-state lighting," *MRS Bull.* **26**, 764–769 (2001).
- B. Arredondo, B. Romero, J. M. Sánchez Pena, A. Fernández-Pacheco, E. Alonso, R. Vergaz, and C. de Dios, "Visible light communication system using an organic bulk heterojunction photodetector," *Sensors* **13**, 12266–12276 (2013).
- P. A. Haigh, F. Bausi, H. Le Minh, I. Papakonstantinou, W. O. Popoola, A. Burton, and F. Cacialli, "Wavelength-multiplexed polymer LEDs: towards 55 Mb/s organic visible light communications," *IEEE J. Sel. Areas Commun.* **33**, 1819–1828 (2015).
- P. A. Haigh, Z. Ghassemlooy, S. Rajbhandari, and I. Papakonstantinou, "Visible light communications using organic light emitting diodes," *IEEE Commun. Mag.* **51**, 148–154 (2013).
- M. T. Sajjad, P. P. Manousiadis, H. Chun, D. A. Vithanage, S. Rajbhandari, A. L. Kanibolotsky, G. Faulkner, D. O'Brien, P. J. Skabara, I. D. W. Samuel, and G. A. Turnbull, "Novel fast color-converter for visible light communication using a blend of conjugated polymers," *ACS Photon.* **2**, 194–199 (2015).
- L. Wang, Z. Wei, C.-J. Chen, L. Wang, H. Y. Fu, L. Zhang, K.-C. Chen, M.-C. Wu, Y. Dong, Z. Hao, and Y. Luo, "1.3 GHz E-O bandwidth GaN-based micro-LED for multi-gigabit visible light communication," *Photon. Res.* **9**, 792–802 (2021).
- S. Zhang, D. Tsonev, S. Videv, S. Ghosh, G. A. Turnbull, I. D. W. Samuel, and H. Haas, "Organic solar cells as high-speed data detectors for visible light communication," *Optica* **2**, 607–610 (2015).
- Y. Xu, J. Chen, H. Zhang, H. Wei, L. Zhou, Z. Wang, Y. Pan, X. Su, A. Zhang, and J. Fu, "White-light-emitting flexible display devices based on double network hydrogels crosslinked by YAG:Ce phosphors," *J. Mater. Chem. C* **8**, 247–252 (2020).
- X. Dai, Z. Zhang, Y. Jin, Y. Niu, H. Cao, X. Liang, L. Chen, J. Wang, and X. Peng, "Solution-processed, high-performance light-emitting diodes based on quantum dots," *Nature* **515**, 96–99 (2014).
- Y.-M. Huang, K. James Singh, A.-C. Liu, C.-C. Lin, Z. Chen, K. Wang, Y. Lin, Z. Liu, T. Wu, and H.-C. Kuo, "Advances in quantum-dot-based displays," *Nanomaterials* **10**, 1327 (2020).
- V. Wood and V. Bulović, "Colloidal quantum dot light-emitting devices," *Nano Rev.* **1**, 5202 (2010).
- X. L. Fan, T. Wu, B. Liu, R. Zhang, H. C. Kuo, and Z. Chen, "Recent developments of quantum dot based micro-LED based on non-radiative energy transfer mechanism," *Opto-Electron Adv.* **4**, 21002201 (2021).
- X. Xiao, H. Tang, T. Zhang, W. Chen, W. Chen, D. Wu, R. Wang, and K. Wang, "Improving the modulation bandwidth of LED by CdSe/ZnS quantum dots for visible light communication," *Opt. Express* **24**, 21577–21586 (2016).
- C.-Y. Kang, C.-H. Lin, C.-H. Lin, T.-Y. Li, S.-W. Huang, C.-L. Tsai, C.-W. Sher, T.-Z. Wu, P.-T. Lee, X. Xu, M. Zhang, C.-H. Ho, J.-H. He, and H.-C. Kuo, "Highly efficient and stable white light-emitting diodes using perovskite quantum dot paper," *Adv. Sci.* **6**, 1902230 (2019).
- Q. V. Le, K. Hong, H. W. Jang, and S. Y. Kim, "Halide perovskite quantum dots for light-emitting diodes: properties, synthesis, applications, and outlooks," *Adv. Electron. Mater.* **4**, 1800335 (2018).
- I. Dursun, C. Shen, M. R. Parida, J. Pan, S. P. Sarmah, D. Priante, N. Alyami, J. Liu, M. I. Saidaminov, M. S. Alias, A. L. Abdelhady, T. K. Ng, O. F. Mohammed, B. S. Ooi, and O. M. Bakr, "Perovskite nanocrystals as a color converter for visible light communication," *ACS Photon.* **3**, 1150–1156 (2016).
- C. Jiang, J. Yao, P. Huang, R. Tang, X. Wang, X. Lei, H. Zeng, S. Chang, H. Zhong, H. Yao, C. Zhu, and T. Chen, "Perovskite quantum dots exhibiting strong hole extraction capability for efficient inorganic thin film solar cells," *Cell Rep. Phys. Sci.* **1**, 100001 (2020).
- P. Ramasamy, D.-H. Lim, B. Kim, S.-H. Lee, M.-S. Lee, and J.-S. Lee, "All-inorganic cesium lead halide perovskite nanocrystals for photodetector applications," *Chem. Commun.* **52**, 2067–2070 (2016).
- S. A. Veldhuis, P. P. Boix, N. Yantara, M. Li, T. C. Sum, N. Mathews, and S. G. Mhaisalkar, "Perovskite materials for light-emitting diodes and lasers," *Adv. Mater.* **28**, 6804–6834 (2016).
- X. Zhang, H. Liu, W. Wang, J. Zhang, B. Xu, K. L. Karen, Y. Zheng, S. Liu, S. Chen, K. Wang, and X. W. Sun, "Hybrid perovskite light-emitting diodes based on perovskite nanocrystals with organic-inorganic mixed cations," *Adv. Mater.* **29**, 1606405 (2017).
- S. Mei, X. Liu, W. Zhang, R. Liu, L. Zheng, R. Guo, and P. Tian, "High-bandwidth white-light system combining a micro-LED with perovskite quantum dots for visible light communication," *ACS Appl. Mater. Interfaces* **10**, 5641–5648 (2018).
- N. Laurand, B. Guilhabert, J. McKendry, A. E. Kelly, B. Rae, D. Massoubre, Z. Gong, E. Gu, R. Henderson, and M. D. Dawson, "Colloidal quantum dot nanocomposites for visible wavelength conversion of modulated optical signals," *Opt. Mater. Express* **2**, 250–260 (2012).
- H. Li, X. Chen, J. Guo, and H. Chen, "A 550 Mbit/s real-time visible light communication system based on phosphorescent white light LED for practical high-speed low-complexity application," *Opt. Express* **22**, 27203–27213 (2014).
- M. Xia, S. Zhu, J. Luo, Y. Xu, P. Tian, G. Niu, and J. Tang, "Ultrastable perovskite nanocrystals in all-inorganic transparent matrix for high-speed underwater wireless optical communication," *Adv. Opt. Mater.* **9**, 2002239 (2021).
- K. James Singh, Y.-M. Huang, T. Ahmed, A.-C. Liu, S.-W. Huang, F.-J. Liou, T. Wu, C.-C. Lin, C.-W. Chow, G.-R. Lin, and H.-C. Kuo, "Micro-LED as a promising candidate for high-speed visible light communication," *Appl. Sci.* **10**, 7384 (2020).
- S.-W. H. Chen, Y.-M. Huang, Y.-H. Chang, Y. Lin, F.-J. Liou, Y.-C. Hsu, J. Song, J. Choi, C.-W. Chow, C.-C. Lin, R.-H. Horng, Z. Chen, J. Han, T. Wu, and H.-C. Kuo, "High-bandwidth green semipolar (20–21) InGaN/GaN micro light-emitting diodes for visible light communication," *ACS Photon.* **7**, 2228–2235 (2020).
- S.-W. H. Chen, Y.-M. Huang, K. James Singh, Y.-C. Hsu, F.-J. Liou, J. Song, J. Choi, P.-T. Lee, C.-C. Lin, Z. Chen, J. Han, T. Wu, and H.-C. Kuo, "Full-color micro-LED display with high color stability using semipolar (20–21) InGaN LEDs and quantum-dot photoresist," *Photon. Res.* **8**, 630–636 (2020).
- S.-W. Huang, C.-C. Shen, T. Wu, Z.-Y. Liao, L.-F. Chen, J.-R. Zhou, C.-F. Lee, C.-H. Lin, C.-C. Lin, C.-W. Sher, P.-T. Lee, A.-J. Tzou, Z. Chen, and H.-C. Kuo, "Full-color monolithic hybrid quantum dot nanoring micro light-emitting diodes with improved efficiency using atomic layer deposition and nonradiative resonant energy transfer," *Photon. Res.* **7**, 416–422 (2019).

31. Y. H. Chang, Y. M. Huang, W. H. Gunawan, G. H. Chang, F. J. Liou, C. W. Chow, H. C. Kuo, Y. Liu, and C. H. Yeh, "4.343-Gbit/s green semipolar (20-21)  $\mu$ -LED for high speed visible light communication," *IEEE Photon. J.* **13**, 7300204 (2021).
32. H. Fu, Z. Lu, X.-H. Zhao, Y.-H. Zhang, S. P. DenBaars, S. Nakamura, and Y. Zhao, "Study of low-efficiency droop in semipolar (20-2-1) InGaN light-emitting diodes by time-resolved photoluminescence," *J. Disp. Technol.* **12**, 736–741 (2016).
33. M. Monavarian, A. Rashidi, A. Aragon, S. Oh, M. Nami, S. DenBaars, and D. Feezell, "Explanation of low efficiency droop in semipolar (20-2-1) InGaN/GaN LEDs through evaluation of carrier recombination coefficients," *Opt. Express* **25**, 19343–19353 (2017).
34. C. Shen, T. Ng, J. Leonard, A. Pourhashemi, S. Nakamura, S. DenBaars, J. Speck, A. Alyamani, M. El-Desouki, and B. Ooi, "High-brightness semipolar (202-1) blue InGaN/GaN superluminescent diodes for droop-free solid-state lighting and visible-light communications," *Opt. Lett.* **41**, 2608–2611 (2016).
35. D.-H. Lee, J.-H. Lee, J.-S. Park, T.-Y. Seong, and H. Amano, "Improving the leakage characteristics and efficiency of GaN-based micro-light-emitting diode with optimized passivation," *ECS J. Solid State Sci. Technol.* **9**, 055001 (2020).
36. M. S. Wong, D. Hwang, A. I. Alhassan, C. Lee, R. Ley, S. Nakamura, and S. P. DenBaars, "High efficiency of III-nitride micro-light-emitting diodes by sidewall passivation using atomic layer deposition," *Opt. Express* **26**, 21324–21331 (2018).
37. Y.-H. Chang, J.-C. Lin, Y.-C. Chen, T.-R. Kuo, and D.-Y. Wang, "Facile synthesis of two-dimensional Ruddlesden–Popper perovskite quantum dots with fine-tunable optical properties," *Nanoscale Res. Lett.* **13**, 247 (2018).
38. L. Zhou, K. Yu, F. Yang, H. Cong, N. Wang, J. Zheng, Y. Zuo, C. Li, B. Cheng, and Q. Wang, "Insight into the effect of ligand-exchange on colloidal CsPbBr<sub>3</sub> perovskite quantum dot/mesoporous-TiO<sub>2</sub> composite-based photodetectors: much faster electron injection," *J. Mater. Chem. C* **5**, 6224–6233 (2017).
39. M. F. Leitão, M. S. Islim, L. Yin, S. Viola, S. Watson, A. Kelly, X. Li, D. Yu, H. Zeng, S. Videv, H. Haas, E. Gu, N. Laurand, and M. D. Dawson, "MicroLED-pumped perovskite quantum dot color converter for visible light communications," in *IEEE Photonics Conference (IPC)* (2017), pp. 69–70.
40. C. Ruan, Y. Zhang, M. Lu, C. Ji, C. Sun, X. Chen, H. Chen, V. L. Colvin, and W. W. Yu, "White light-emitting diodes based on AgInS<sub>2</sub>/ZnS quantum dots with improved bandwidth in visible light communication," *Nanomaterials* **6**, 13 (2016).
41. H. Cao, S. Lin, Z. Ma, X. Li, J. Li, and L. Zhao, "Color converted white light-emitting diodes with 637.6 MHz modulation bandwidth," *IEEE Electron Device Lett.* **40**, 267–270 (2019).
42. M. Leitão, M. Islim, L. Yin, S. Viola, S. Watson, A. Kelly, Y. Dong, X. Li, H. Zeng, S. Videv, H. Haas, E. Gu, I. Watson, N. Laurand, and M. Dawson, "Pump-power-dependence of a CsPbBr<sub>3</sub>-in-Cs<sub>4</sub>PbBr<sub>6</sub> quantum dot color converter," *Opt. Mater. Express* **9**, 3504–3518 (2019).
43. C. Yeh, Y. Liu, and C. Chow, "Real-time white-light phosphor-LED visible light communication (VLC) with compact size," *Opt. Express* **21**, 26192–26197 (2013).